Process and realization of a three-dimensional gold electroplated antenna on a flexible epoxy film for wireless micromotion system

Philippe Basset and Andreas Kaiser
Institut d'Electronique et de Microélectronique du Nord, IEMN, UMR CNRS 8520, Cité scientifique, Avenue Poincaré, -B.P. 69, F-59652 Villeneuve D'Ascq Cedex, France

Dominique Collard
CIRMM/IIS-CNRS—Institut of Industrial Sciences, The University of Tokyo, Tokyo, Japan

Lionel Buchaillot[a)]
Institute d'Electronique et de Microélectronique du Nord, IEMN, UMR CNRS 8520, Cité scientifique, Avenue Poincaré, -B.P. 69, F-59652 Villeneuve D'Ascq Cedex, France

The process and realization of a light and low resistive antenna for wireless communications by inductive coupling at 13.56 MHz is presented. The antenna is realized on an insulated substrate made of SU-8 resist in order to prevent the losses due to eddy currents from occurring and to strongly decrease its weight. The conductor is obtained by electroplating 24 μm of gold in a mold of AZ-4562 resist. A Q factor of 29 has been obtained with a maximum of 37 at 19 MHz, for antenna dimensions of 1.5×1.5 cm^2. This antenna is the key component for a wireless power supplied microrobot. © *2002 American Vacuum Society.* [DOI: 10.1116/1.1494066]

I. INTRODUCTION

The use of the inductive coupling properties has increased considerably in the last ten years. They allow not only the remote feeding of electronic circuits but also the exchange of information between the power source and an inboard device. The major part of the application relates to the radio frequency identification and is widespread in the industry. Inductive powering and telemetry are also widely used in the fields of sensors. One finds many applications in the medical domain with, for instance, the possibility of carrying out permanent implants checking different parameters (like insulin rate and intraocular pressure),[1] or to activate specific nerves.[2,3] In the same way, automotive industry develops devices providing the real time pressure of tires by inductive coupling to an inboard computer.

However, remote power feeding and simultaneous remote control, namely remote actuation, in order to have a wireless microrobot, is a field which remains unexplored. This kind of micromachine could be very useful for industrial inspection and self-repairing of complex equipment.[4] Depending on the type of actuation principle, the required power can be of the order of several hundreds of mW.[5,6] Moreover, most of the micromotion systems are not able to support more than their own weight, requiring new design concepts.

Several micromachined antennas for remote powering by inductive coupling were already realized.[7–9] But only a hundred mW were transmitted at frequencies lower than 5 MHz. This article reports the development and the realization of a micromachined antenna from which we transmitted, to a distance of 1 cm, up to 1.25 W at the frequency of 13.56 MHz. This result has been obtained thanks to the realization of the antenna on an insulating epoxy substrate. Thus, no loss due to eddy currents occurs. Moreover, the parasitic capacitance of the inductance is reduced considerably, pushing back its self-resonance frequency largely beyond our operating frequency. Lastly, for the application of our autonomous microrobot,[10] the use of epoxy instead of silicon decreases the weight supported by the microsystem actuators.

II. PROCESS

The process flow of the antenna fabrication is shown in Fig. 1. First, a 2 μm low-temperature oxide was deposited on a silicon wafer and subsequently used as a sacrificial layer. Then, 150 μm of epoxy-type resist SU-8 is spun up. This film, once polymerized, becomes a flexible, tough, and light substrate. The conductor is made of thick electroplated gold. So, a seed layer of nickel is sputtered in order to achieve the electrolysis. A 30 μm thick mold of positive resist AZ 4562 is realized and followed by gold plating. Finally, the mold is removed, the seed layer of nickel is etched by nitric acid, and the SU-8 film is separated from the silicon using hydrofluoric acid.

A. SU-8 process

SU-8 is a negative near-UV (365 nm wavelength) photoresist, originally developed by IBM.[11,12] Its low optical absorption in the UV spectrum allows for layers thicker than 1 mm.[13] Since the SU-8 is very sensitive to the variation of the process parameters, the process is detailed in the following sections.

1. Spinning and prebake

First, the substrate is baked in an oven at 170 °C for 30 min to ensure good dehydration. Then, 5 ml of SU-8 100 resist are dispensed with a cut-end pipette on a 3 in. wafer. Spread and coat are performed on a conventional spincoater with a slow acceleration of 200 rpm^2 in order to avoid the
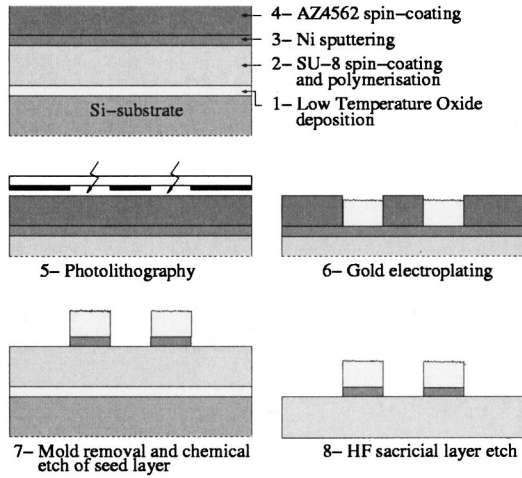
FIG. 1. Process flow for the realization of the antenna.

formation of an air gap.[14] The spread cycle consists of six coats from 500 to 1000 rpm, of 60 s each. The final coat, in order to obtain a 150 μm film, is performed at 2500 rpm for 30 s, with an acceleration of 500 rpm^2 in order to improve the uniformity of the film.

An intermediate bake of 3 min at 65 °C is performed to limit the stress in the resist. It is followed by a prebake of 30 min at 95 °C on a hot plate in order to remove the solvents and to planarize the film (the glass temperature of the SU-8 is about 55 °C).

2. Exposure and postexposure bake

The wafer is exposed with a mercury flash UV lamp (355, 405, and 436 nm) at 15 mJ/cm^2 for 60 s. During the postexposure bake, 15 min at 95 °C on a hot plate, the volume of the resist reduces and its density increases. This shrinkage brings about stress, mainly during the cooling phase.[15] In
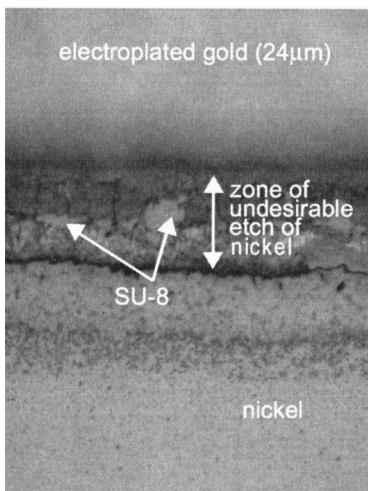

FIG. 2. Top view picture showing undesirable chemical etch of nickel during gold plating.
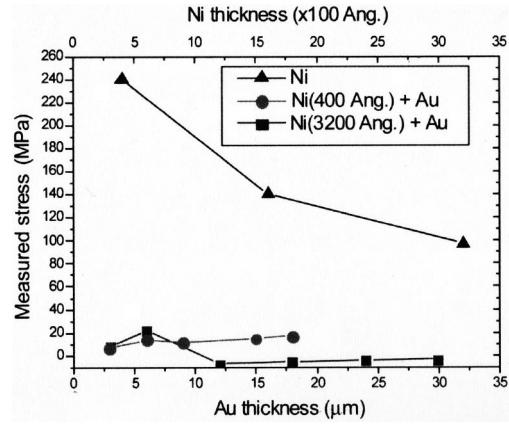

FIG. 3. Evolution of stress of sputtered nickel and plated gold for different thickness.

order to control the cooling of the substrate and to avoid cracks or excessive stress, a last bake of 3 min at 65 °C is subsequently performed.

3. Seed layer

In order to allow the reduction of gold ions on the substrate and to realize the three-dimensional structures by electroplating, a conductive seed layer is deposited on the SU-8 film. This is achieved by sputtering a 3000 Å nickel layer. It was noted that during the electroplating and under the effect of chemical substances from the resist mold, Ni is strongly affected at the resist/Au interface (Fig. 2). A 500 Å deposit of Ni limits the gold thickness to 8 μm. Beyond 8 μm, 200 μm wide nickel patterns are etched by the electrolyte during the plating. Then, the gold begins to peel. A stress calculation according to the thickness of nickel shows that the Ni film is strongly in tension and that the stress decreases as the Ni thickness increases. On the other hand, after a few microns of gold electroplating, the stress of the Ni–Au layer decreases and remains stable (Fig. 3). The study was made on three 2 in. wafers. The stress values are obtained from the wafer radius of curvature measurement and the formula of Stoney:
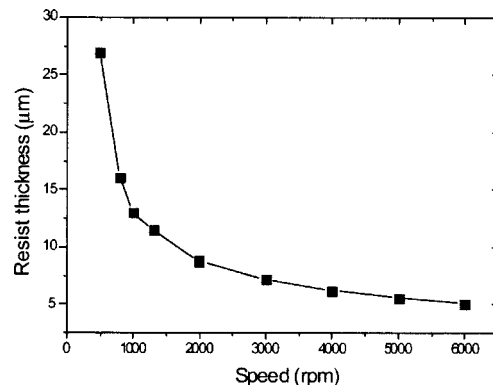

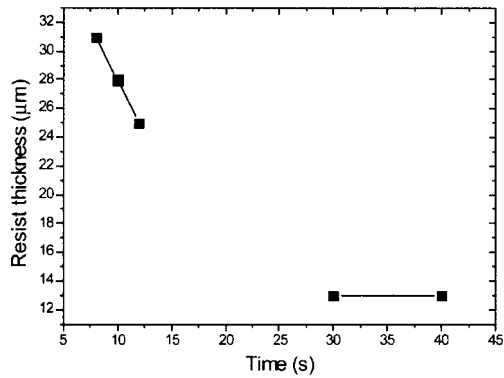FIG. 4. Spin coating calibration for AZ-4562 (time=30 s).

FIG. 5. Spincoating curves for AZ-4562 at the constant speed 1000 rpm.

FIG. 6. Influence of nitrogen outgassing on thick positive photoresist.

$$\sigma = \frac{E}{1-\nu} \cdot \frac{t_s^2}{6 \cdot t_f} \cdot \left(\frac{1}{\rho} - \frac{1}{\rho_0} \right), \qquad (1)$$

where E is the Young's modulus, ν is the Poisson coefficient, t_s is the substrate thickness, t_f is the film thickness, and ρ_0 and ρ are, respectively, the radius of curvature of the wafer before and after the film deposition.

4. Mold process

The mold for the electroplated structures is fabricated with the positive photoresist HOECHST AZ-4562. The main advantages of this resist are that the process can be performed with a standard setup for UV lithography, and it is easily removed compared to epoxy-based molds.

5. Spinning

First, hexamethyldisilazane promoter is spun up at 3500 rpm. Next, 7.5 ml of AZ-4562 is spread over the substrate and spincoated with a rotating cover spinner. Thanks to this equipment which prevents the evaporation of the solvent and minimizes the air turbulence effects,[16] a thickness of 30 μm is obtained in a single step. The spin velocity and acceleration were selected as a compromise between good uniformity of the resist film (high speed and acceleration) and minimal stress (low speed and acceleration). Figure 4 shows the resist thickness according to the spinning velocity for a 30 s coating time. A speed of 1000 rpm is selected by assuming that the intersection of the two asymptotes of the curve is a good compromise. Thanks to Fig. 5, relating the resist thickness to
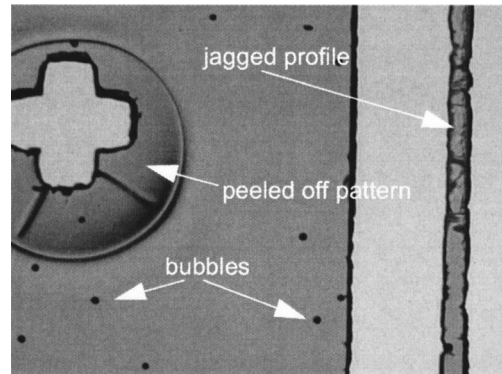
the spinning time for a 1000 rpm spinning speed, a 30 μm thickness is achieved by selecting a spinning duration of 8 s.

6. Prebake

A prebake is performed to remove most of the solvent. A prebake in an oven leads to a slow bake which prevents the resist from drying too fast and the solvent from being trapped, leading to bubble growth and resist cracking or peeling. A possible drawback is the formation of a crust atop of the resist surface after a too long bake. Hot plates avoid crust formation by heating from the rear side, but if one is not using temperature controlled plates, great temperature contrast induces strong mechanical stress[17] and the resist tends to flow toward the center of the wafer. For instance, we have observed, after development, a 5 μm peeling at the edge of the patterns for a prebake of 30 min on a hot plate at 70 °C.

Due to the low speed and the coating time, a large quantity of the solvent remains in the resist. So, just after spinning, the wafer is kept at room temperature for 15 min to allow most of the solvent to evaporate.[18] Multiple attempts lead us to use both oven and hot-plate bakes: 1 h in an oven at 50 °C followed by 10 min on a hot plate at 110 °C.

7. Exposure and development

A lack of water results in cracking during the exposure.[16] Therefore, in order to allow the resist rehydration, a 15 min wait was observed between the prebake and the exposure.

During the exposure, the absorption of the photoactive compound decreases due to its conversion in carboxylic acid.[19] Thus, exposure dose increases drastically with resist thickness. An energy of about 2500 mJ/cm^2 is required to expose the resist. Exposing at this energy with an ordinary
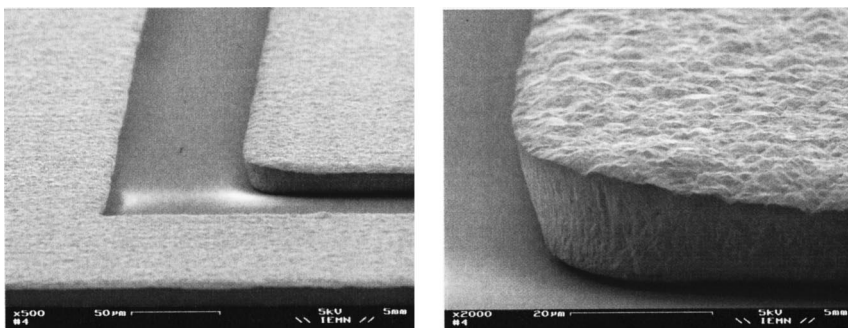

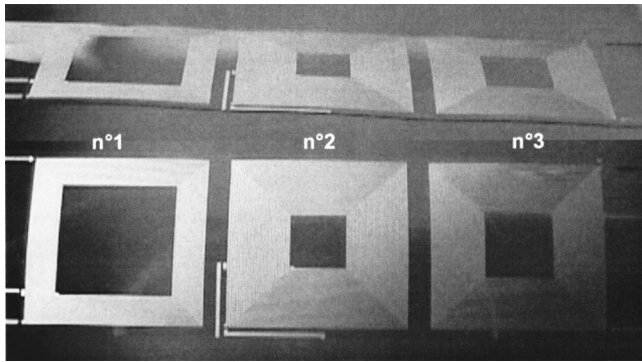FIG. 7. Electroplated gold on SU-8, 24 μm in thickness.

FIG. 8. Overview of antennas. Outer diameter: 15 mm. Space between turns: 100 μm. Antenna 1: 16 turns of 62.5 μm width. Antenna 2: 26 turns of 100 μm width. Antenna 3: 23 turns of 100 μm width.

FIG. 9. Amplitude and angle of antenna impedance.

high-pressure mercury lamp heats up the resist, resulting in stress increasing and the development of unexposed parts as well. Outgassing of nitrogen occurs and has a two-fold consequence; it has no time to diffuse and remains in the resist inducing peeling of the smallest patterns, and it creates microholes in the exposed parts of the resist resulting in a jagged profile of the patterns after development (Fig. 6). These phenomena can be limited by two ways: by decreasing the mercury lamp power (with a 400 nm filter for instance) and increasing the exposure time, or by alternating short exposures with long pauses. Immersion development is carried out by using a potassium-based alkaline developer (Hoechst AZ 400K)/water, 1:4 in volume.

8. Postbake

The postbake increases the resist adhesion on the substrate during the electrolysis, and partially destroys the photoactive compound in the nonexposed areas. Therefore, it limits a chemical reaction with the plating solution.[20,21] However, high-temperature baking causes the resist to flow and the aspect ratio of the structures becomes very low. To reduce the flowing and shrinking, the postbake temperature is set to 95 °C for 1 min on a hot plate.[22] However, the larger
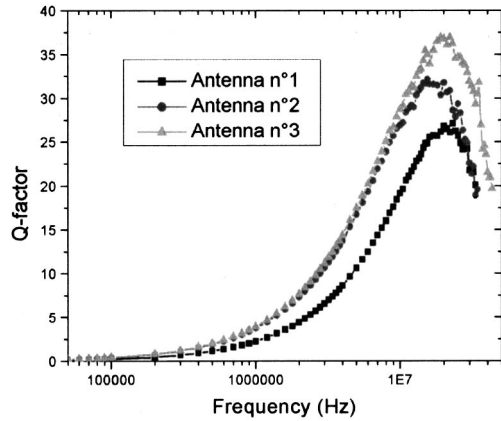
the planar area of the remaining photoresist, the larger the distortion of the pattern, and the mask has to be designed consequently.

B. Electroplating

Gold is electroplated using a commercially available neutral gold cyanide solution. Many parameters influence the deposit.[23] The high temperature of the electrolyte and the current density increase the deposition rate but also increase the roughness, resulting in ohmic losses. The adherence of the resist is also affected by the bath temperature.[24] Consequently, a deposition rate of 0.2 μm/min during 2 h was selected yielding a 24 μm electroplated gold layer (Fig. 7). The bath temperature was set to 45 °C.

The duration of the plating induces hard crosslinking of a thin film of resist which is impossible to remove with acetone or oxygen plasma. Subsequently, the seed layer is not isotropically etched, because of the protection of the residual resist film. When this occurs, the nickel under the structures is totally etched before all the undesired areas have been removed, and the gold patterns lift off. A good way to totally remove the mold is to dip the wafer in the AZ 400 developer
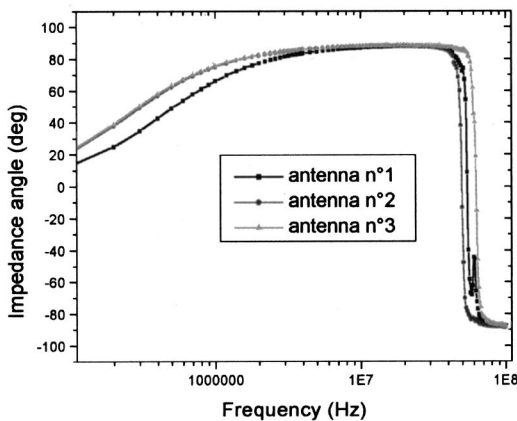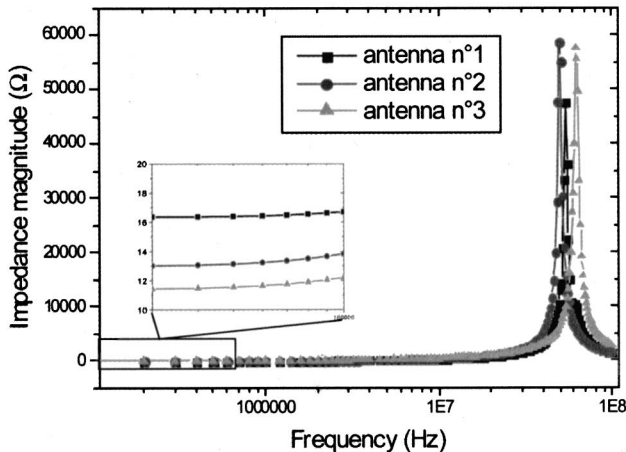

FIG. 10. *Q* factor of antennas, extracted from Agilent 8753ES Network Analyzer measurements.

TABLE I. Characteristics of receiver antennas.

	Antenna 1	Antenna 2	Antenna 3
L (μH)	5.8	7.8	7.2
Self-resonance frequency (MHz)	54	49	62
C (pF)	1.5	1.3	0.92
Q_L (13.56 MHz)	19	27	29
Q_L max	27 (27 MHz)	32 (15.5 MHz)	37 (19 MHz)

heated to 80 °C for 30 min. Afterward, the nickel can be easily etched with nitric acid diluted by 4 volumes of deionized water and heated at 40 °C. Finally, the wafer is dipped for 5 min in an ultrasonic bath and the sacrificial oxide is etched with HF.

III. EXPERIMENTAL RESULTS

Three hollow coil antennas with different designs have been fabricated and released from the silicon substrate (Fig. 8). The outer diameter d_o of the coils is 15 mm and the space between the gold turns is 100 μm. The turn number of antennas referenced 1, 2, and 3 are, respectively, 16, 26, and 23, and the conductor widths are 62.5, 100, and 100 μm.

A. Measurement and *Q*-factor extraction

Antenna testing was performed with an Agilent 8753ES Network Analyzer. One-port S parameters were measured from 30 kHz to 100 MHz and converted to impedance Z_L. Then, the capacitive parasitic C_p of the test device was de-embedded using open calibration of the device. Parameter extraction is deduced from an equivalent circuit consisting of a capacitor C in parallel with an inductance L in series with a resistor R. Extraction of L and C requires the following assumptions: as frequency increases, the penetration of the magnetic field into the conductor is attenuated (skin effect), which causes a reduction in the magnetic flux internal to the conductor. However, L does not decrease significantly with increasing frequency because it is predominantly determined by the magnetic flux external to the conductor.[25] Thus, L can be approximated as constant with frequency. C is considered independent of frequency since it represents the metal-to-metal overlap capacitance between the turns. L is extracted from the low-frequency imaginary part of Z_L and C is extracted using the low-frequency L value and the resonant frequency of the antenna. The quality factor Q_L (Fig. 9) is estimated by taking the ratio of the imaginary and real components of the one-port impedance, observing Z_L is purely inductive at our frequencies of interest (Fig. 10).

The results are reported in Table I. The maximum Q factor is obtained for antenna 3. Even though the design of antenna 2 has a larger inductive value, the lower Q factor can be explained by the fact that inner turns increase serial losses without having a high contribution to the inductance. The main advantage of using an insulating substrate is that the parasitic capacitance is very low, which leads to self-resonance frequencies around 30 MHz. Hence, a high transmitter frequency can be used, allowing a better Q. If using a
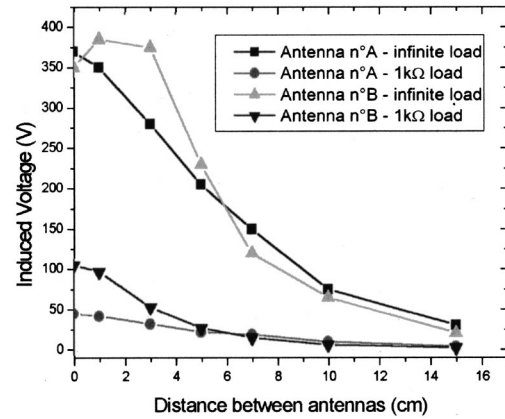

FIG. 11. Measured peak to peak induced voltage on Antenna 3 tuned at 13.56 MHz with two transmitter antennas. Antenna A: Two turns, 14 cm diameter. Antenna B: Four turns, 7 cm diameter.

silicon substrate with a SiO$_2$ layer, the thickness of the dielectric should have been higher than 100 μm to be able to work at 13.56 MHz.

B. Energy transfer experiment

At the emission, an electronic card is able to supply an ac current up to 1 A/18 V through a transmitter antenna made of a copper wire of 1 mm diameter. The card is controlled by a computer that modulates the current amplitude in real time. The receiver antenna is tuned to the operating frequency of 13.56 MHz with a discrete capacitor. The induced voltage as a function of distance for two transmitter antennas is reported in Fig. 11. 1.25 W have been transmitted to a 1 kΩ load at a distance of 1 cm. Dimensions of the transmitter antenna have a serious effect on the induced power. Reducing its diameter increases the received voltage but only for small distances since the coupling factor is then closer to 1. For high coupling (e.g., small transmitter antenna diameter and very short distances of transmission), we notice that the induced voltage on the infinite load decreases. It can be explained by the fact that the 2 poles of the emitter and receiver LC-tanks do not match the transmitter frequency anymore.

IV. CONCLUSION

We have presented a complete and low-cost process to realize high inductive value and low resistive antenna for inductive coupling and remote powering applications. Inductance of 7.2 μH with a maximum Q factor of 37 at 19 MHz has been fabricated with dimensions of 1.5×1.5 cm^2. Conductors are made of 24 μm electroplated gold thanks to a positive photoresist AZ-4562 mold. The use of an epoxy substrate drastically reduces eddy currents, parasitic capacitance, and the weight of the antenna. 1.25 W have been transmitted to a 1 kΩ load at 13.56 MHz. These components are suitable for a wireless micromotion systems.

[1] R. Puers, G. Vandevoorde, and D. De Bruyker, J. Micromech. Microeng. **10**, 124 (2000).

[2] T. Akin, K. Najafi, and R. M. Bradley, J. Solid State Circ. **33**, 109 (1998).

[3] W. Liu, K. Vichienchom, M. Clements, S. C. DeMarco, C. Hughes, E. McGucken, M. S. Humayun, E. de Juan, J. D. Weiland, and R. Greenberg, J. Solid State Circ. **35**, 1487 (2000).

[4] M. Takeda, Proceedings of the IEEE MEMS'01, Interlaken, Switzerland, 2001, pp. 182–191.

[5] M. Ataka, A. Omodaka, N. Takeshima, and H. Fujita, J. Microelectromech. Syst. **2**, 146 (1993).

[6] T. Ebefors, J. U. Mattsson, and E. Kälvesten, J. Micromech. Microeng. **10**, 337 (2000).

[7] J. A. Von Arx and K. Najafi, Proceedings of Transducers'97, Chicago, IL, 1997, pp. 999–1002.

[8] D. Dudenbostel, K.-L. Krieger, C. Candler, and R. Laur, Proceedings of Transducers'97, Chicago, IL, 1997, p. 995.

[9] S. Takeuchi, N. Futai, and I. Shimoyama, Proceedings of the of IEEE MEMS'01, Interlaken, Switzerland, 2001, pp. 574–577.

[10] P. Basset, A. Kaiser, P. Bigotte, D. Collard, and L. Buchaillot, Proceedings of MEMS'02, pp. 606–609.

[11] J. M. Shaw, J. D. Gelorme, N. C. LaBianca, W. E. Conley, and S. J. Holmes, IBM J. Res. Dev. **41**.

[12] K. Y. Lee, N. LaBianca, S. A. Rishton, S. Zolgharnain, J. D. Gelorme, J Shaw, and T. H. P Chang, J. Vac. Sci. Technol. B **13**, 3012 (1995).

[13] S. Arscott, F. Garet, P. Mounaix, L. Duvillaret, J. L. Coutaz, and D. Lippens, Electron. Lett. **35**, 243 (1999).

[14] Microlithography Chemical Corp., application notes (1997).

[15] H. Lorenz, M. Despont, N. Fahrmi, J. Brugger, P. Vettiger, and P. Renaud, Sens. Actuators A **64**, 33 (1998).

[16] S. Roth, L. Dellmann, G.-A. Racine, and N. F. deRooij, J. Micromech. Microeng. **9**, 105 (1999).

[17] B. Loechel, J. Micromech. Microeng. **10**, 108 (2000).

[18] Hoechst Celanese Corporation, Standard Photoresist AZ 45000 series—Technical notes (1994).

[19] V. Conedera, N. Fabre, and M. Dilhan, J. Micromech. Microeng. **7** (1997).

[20] H. Miyajima and M. Mehregany, J. Microelectromech. Syst. **4**, 220 (1995).

[21] J. Gobet, F. Cardot, J. Bergqvist, and F. Rudolf, J. Micromech. Microeng. **3**, 123 (1993).

[22] G. Engelmann and H. Reichl, Microelectron. Eng. **17**, 303 (1992).

[23] J. W. Dini, *Electrodeposition, The Materials Science of Coating and Substrates* (Noyes, Park Ridge, NJ, 1992).

[24] S. Boret, Ph.D. thesis (in French), Université des Sciences et Technologies de Lille, 1999.

[25] C. P. Yue and S. S. Wong, J. Solid State Circ. **33**, 743 (1998).